



Influence of Seismic Design Evolution on the Seismic Collapse Behavior and Losses of Prototype Steel Buildings with Moment-Resisting Frames

Tung-Yu Wu, Ph.D., M.ASCE¹; Sherif El-Tawil, Ph.D., P.E., F.ASCE²; and Jason McCormick, Ph.D., P.E., M.ASCE³

Abstract: Seismic design provisions for steel moment frame buildings have undergone substantial changes over the past half century. Despite the anticipated benefits of enforcing newer codes, it is not yet fully known how the evolution of seismic provisions has changed the risk associated with steel moment frame use. To address this shortcoming, a seismic loss assessment is performed for two-, four, and eight-story prototype steel moment frames designed using seismic provisions from three eras spanning the past half century. Frames of different vintages differ significantly in material properties, welding practices, connection types, seismic lateral force used for design, and panel zone design philosophy. High-fidelity models capable of explicitly capturing instabilities and fracture are employed to determine the effect of the differences in these designs. The simulation results show that although the collapse risk decreased as the codes evolved, the collapse probability of frames designed to the latest specifications still exceed the expected norms. Analysis of the four-story frames showed that the effect of brittle fracture in the welds of pre-Northridge connections on frame collapse capacity is modest. However, it is quite influential on economic and social losses for the level of seismic hazard considered. The assessment results are used to propose strategies for reducing the seismic losses of communities with steel buildings. **DOI:** 10.1061/(ASCE)ST.1943-541X.0002743. © 2020 American Society of Civil Engineers.

Introduction

Seismic design practices for buildings have experienced substantial changes over the past half century. Major changes to seismic codes typically happen in response to unexpected building damage as a result of earthquake events with the intent of achieving better building performance during future events (SEAOC Seismology Committee 2009). For example, after the 1971 San Fernando earthquake, the number of seismic zones was increased from four to five and a coefficient, S, accounting for the effect of soil-structure interaction was introduced, leading to a better characterization of the seismic demands on buildings. After the 1985 Mexico City earthquake, requirements for irregular structures and building separation were added to the codes to ensure a more accurate strength distribution and to avoid pounding. Additional changes were made in the 1990s to consider soil liquefaction and near-fault effects due to the widespread ground failure and significant damage around the epicenter of the 1994 Northridge earthquake.

As with other types of construction, seismic design provisions for steel moment–resisting frames (MRF) have evolved substantially during the past 50 years. Steel MRFs have been widely used in areas of high seismicity for decades because of their architectural

Note. This manuscript was submitted on October 3, 2019; approved on March 12, 2020; published online on June 25, 2020. Discussion period open until November 25, 2020; separate discussions must be submitted for individual papers. This paper is part of the *Journal of Structural Engineering*, © ASCE, ISSN 0733-9445.

flexibility, large strength-to-weight ratio, and considerable ductility. The evolution of provisions for steel MRFs can be roughly split into three eras (Uang and Bruneau 2018): (1) prior to 1988; (2) 1988–1997; and (3) 1997–present. The first era corresponds to early seismic practices. The second era incorporates lessons learned during the 1985 Mexico City earthquake, while the last era integrates knowledge gleaned from the 1994 Northridge earthquake.

It is naturally expected that steel buildings designed according to newer codes should have progressively better seismic performance than those designed to older codes. While some studies have investigated how steel buildings designed in different eras have performed (e.g., FEMA 2010; Kircher 2003; Ellingwood et al. 2007; Noroozinejad Farsangi et al. 2016; Hutt et al. 2019), it is difficult to confirm this expectation because the studies used different frame configurations and many were done using computational tools with limited capabilities. For example, most of the studies, including the aforementioned ones, modeled frame response using beam-column elements, which cannot accurately capture the effects of local buckling and their synergistic interactions with the global buckling response of steel members. In addition, most previous studies did not tie the evolution of steel frame design provisions to losses due to component damage resulting from their seismic performance. To address these shortcomings, collapse analysis and seismic loss assessment are performed for a set of prototype steel moment frames that have the same building configuration and site conditions but are designed using seismic provisions from the three eras. The study accounts for major differences in the evolution of seismic design and construction practices over the 50-year period, including material properties, welding practices, connection types, seismic design force requirements, and panel zone design philosophies. The behavior of column splices is, however, not considered in this study due to the lack of experimental information required to characterize it and findings in Stillmaker et al. (2017) suggest that splice fractures did not exacerbate structural response or trigger collapse in the frames they studied.

¹Assistant Professor, Dept. of Civil Engineering, National Taiwan Univ., Taipei 10617, Taiwan (corresponding author). ORCID: https://orcid.org/0000-0002-2981-1910. Email: tungyuwu@ntu.edu.tw

²Professor, Dept. of Civil and Environmental Engineering, Univ. of Michigan, Ann Arbor, MI 48109-2125. Email: eltawil@umich.edu

³Associate Professor, Dept. of Civil and Environmental Engineering, Univ. of Michigan, Ann Arbor, MI 48109-2125. Email: jpmccorm@umich.edu

Three prototype SMRFs that are two-, four-, and eight-stories are considered to account for the effect of building height. High-fidelity models capable of explicitly capturing fracture and a full range of local and global instabilities are employed in the assessment. The collapse capacity of the frames is computed using incremental dynamic analysis (IDA), as outlined in Vamvatsikos and Cornell (2002), and then combined with the seismic demands to estimate economic (i.e., repair cost and time) and social (i.e., casualties) losses of the frames under a 475-year return period earthquake based on FEMA P-58 methodology. The assessment results are used to propose strategies for reducing the seismic losses of communities with steel buildings.

Evolution of Seismic Design Criteria for Steel MRFS

Seismic Design Forces

Prior to the 1960s, the seismic design force (a laterally applied load) was simply a function of the number of building stories and seismic zone where the building was located. Starting with the 1961 Uniform Building Code (UBC) (ICBO 1961), the spectral shape used to compute the design force became a function of fundamental vibration period (T_1) of the building. The applied force also was adjusted by other coefficients including the system factor in the 1961 UBC and soil profile coefficient in the 1976 UBC (ICBO 1976). The number of seismic zones, which are used to determine the magnitude of spectral shape, increased from four to five in the 1976 UBC and then to six in the 1988 UBC (ICBO 1988). The concept of numbered zones was eventually replaced with seismic hazard contour maps that combine probabilistic maps with deterministic maps since the 1998 version of ASCE 7 (ASCE 1998). The spectral shape evolved as a function of the fundamental period, T_1 . An upper limit on T_1 was not imposed until the 1988 UBC.

The effect of the soil profile at a building site on the design seismic force was first recognized in the 1976 UBC using equations representing soil-structure interaction. In the 1988 UBC, the equations were replaced with four site coefficients (S_1 to S_4) that depended on the soil properties. These coefficients were eventually replaced with a set of earthquake-level dependent site classes (A to F) starting with the 1997 UBC (ICBO 1997).

The system factor (K) was used in the 1961 UBC to consider the effect of system ductility for four types of structural systems. The 1967 UBC (ICBO 1967) introduced ductile moment-resisting space frames and specified additional requirements for buildings in high seismic areas. In the 1988 UBC, the system factor was succeeded by the response modification factor (R_w). Special moment frames were also introduced at this time along with special detailing, as described later. The R_w factor was replaced with the R factor, which approximately equals to $R_w/1.4$, in the 1997 UBC because of the conversion from working stress design to strength design (SEAOC 2009).

Fig. 1 shows a comparison of the equivalent static lateral forces as specified by different codes for steel moment frames (ductile or special, i.e., K = 0.67 for 1961 and 1976 UBC, $R_w = 12$ for 1988 UBC, and R = 8 for ASCE 7-05) located in Santa Monica (34.000, -118.450). The site class is assumed to be D in the ASCE 7-05 (ASCE 2005), which approximately corresponds to soil profile type S_2 in older codes (Dobry et al. 2000). The importance factor is assumed to be 1.0. While Fig. 1 suggests that newer codes generally require larger seismic design forces, ASCE 7-05 uses a smaller response modification factor (i.e., R) due to the implementation of strength design. As a result, at this particular site, all codes have somewhat similar seismic demands due to the adoption of similar

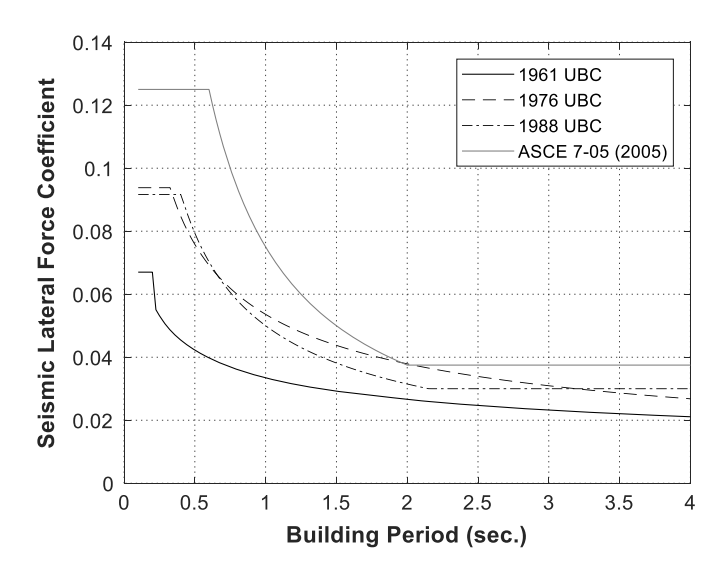


Fig. 1. Minimum seismic lateral force required in different editions of the building codes.

spectral shapes and minimum required forces except the 1961 UBC, which had a substantially lower estimate of seismic hazard.

Design Principles of Steel Moment Frames

The 1961 UBC (ICBO 1961) defined a moment resisting space frame as one able to resist 100% of a building's lateral force and that had a system factor K=0.67. In 1967, a new term, ductile moment resisting space frame, was introduced to differentiate between frames with different levels of ductility. According to the 1970 UBC (ICBO 1970), these frames had: (1) moment connections capable of developing the full plastic capacity of the beams, and (2) minimum slenderness ratios in plastic hinge zones to control local buckling. The 1988 UBC addressed special moment resisting frames for the first time and had a section specifying detailing requirements for this type of system, which is currently used in seismic zones worldwide. The term special implied compliance with criteria for: (1) the strong column-weak beam (SCWB) design principle, (2) stability bracing, and (3) a specific panel zone design philosophy.

The purpose of the SCWB principle is to control inelasticity in columns and retain structural stability, while dissipating energy through beam yielding. This principle is achieved by requiring a flexural strength that is higher for columns than for beams for any moment connection, as stated in the 1988 UBC

$$\sum Z_{c}(F_{yc} - P_{ac}/A_{g}) / \sum Z_{b}F_{yb} > 1.0$$
 (1)

where Z_c and Z_b (or Z_{RBS} if reduced beam sections are used) = plastic section modulus of the columns and beams, respectively; F_{yc} and F_{yb} = specified minimum yield stress of the columns and beams, respectively; and P_{ac} = required compressive strength using the allowable stress design (ASD) load combinations. As can be seen in Eq. (1), material overstrength was not considered. This was a weakness of past seismic provisions because material overstrength was identified as one of the major issues in the 1994 Northridge earthquake. Eq. (1) was subsequently modified in the 1997 AISC seismic provisions (AISC 1997)

$$\sum Z_c(F_{yc} - P_{uc}/A_g) / \sum 1.1 R_y Z_b F_{yb} + M_{uv} > 1.0$$
 (2)

where P_{uc} = required compressive strength using LRFD load combinations; R_y = ratio of the expected yield stress to the specified minimum yield stress; and M_{uv} = additional moment due to shear amplification from the location of the plastic hinge to the column centerline, based on LRFD load combinations. The principle became even more stringent with the 2010 AISC seismic provisions (AISC 2010) because P_{uc} had to include the amplified seismic load. Along with tightening of the SCWB concept, column axial strength criteria also became more severe. For example, the 1988 UBC also required columns to resist an amplified seismic load to address column failures observed in the 1985 Mexico City earthquake.

It was not until the 1988 UBC that column flanges at beam-to-column connections had to be laterally braced at the top and bottom beam flanges unless the column remained elastic. In such cases, lateral bracing had to be provided at only the top beam flanges. Columns were considered to remain elastic if the ratio of column-to-beam moment capacities was more than 1.25. The ratio was increased to 2.0 in the 2002 AISC seismic provisions (AISC 2002). Beam bracing criteria also evolved. Beam flanges were required to be laterally supported with a maximum unbraced length (L_b) of $96r_y$ in the 1988 UBC, where r_y is the radius of gyration about the minor axis. In the 1990 AISC provisions (AISC 1990), L_b was decreased to 2,500 r_y/F_{yb} , a value that has been used since.

Panel zone design philosophy evolved considerably over the years. Prior to 1988, panel zones were designed to remain elastic during seismic events, i.e., a strong panel zone. In this context, strong refers to the fact that the panel zones are stronger than the connecting beams, which mainly contribute to energy dissipation in this approach. The strong panel zone requirement was replaced in the 1988 UBC with a diametrically opposite approach: a weak panel zone, designed to allow most of energy dissipation to occur in the panel zones. Weak panel zones, however, proved problematic during the 1994 Northridge earthquake. The kink in the column flanges that resulted from excessive panel zone distortion was widely thought to be one of the reasons for the widespread connection failures that occurred during that event. This outcome led to the development and specification of a new approach, i.e., balanced panel zone design, which first appeared in the 2002 AISC seismic provisions.

Evolution of Practices for Steel MRFS

In addition to the changes in design criteria, design practices also evolved, influenced by developments in manufacturing and construction technology and a push to minimize design effort and construction costs. Key changes occurred in the properties of structural steel, type of connections, structural systems, and column section selection.

Steel material strength has increased significantly since the 1940s (Coons 1999), when mild structural steel was sold as A7 steel with a specified minimum yield stress $F_y=228$ MPa (33 ksi) (Roeder 2000). Starting in 1961, A36 steel with $F_y=248$ MPa (36 ksi) was incorporated in the AISC specification (AISC 1961) and dominated the market until around the 1994 Northridge earth-quake. A572 Grade 50 steel with $F_y=345$ MPa (50 ksi), which was also a popular option, was sold after the 1969 AISC specification (AISC 1969). A36 steel fell out of favor because its actual yield strength was much higher than its nominal yield strength due to the use of recycled scrap steel, as can be seen from the survey by Coons (1999). In the late 1990s, A992 steel with $F_y=345$ MPa became widely used for wide flange sections because its yield to ultimate strength ratio was constrained (Bartlett et al. 2003).

Connection types as well as weld details changed significantly after the 1994 Northridge earthquake. These changes were documented in the FEMA 350 series of documents (FEMA 2000a). Unlike the welded-flange-bolted-web (WFBW) connections, i.e., pre-Northridge connections from the 1970s, post-Northridge connections incorporated recommendations to avoid early brittle fracture in welds and provide sufficient plastic rotational capacity. Key requirements pertained to the use of filler metal with sufficient Charpy V-Notch (CVN) toughness, removal of the bottom weld backing bar, improved geometry of the weld access hole, and new connection types other than WFBW connections. The most popular type of post-Northridge connection is the reducedbeam-section connection (RBS). This connection type enables beams to yield in the reduced area located at a distance from the column face to reduce the demands on beam-column welds and protect the connection.

Significant changes in the frame configuration used in steel buildings occurred around the mid-1970s and dominated the design practice since the 1980s (FEMA 2000b). The high cost of field-weld moment connections prompted engineers to minimize their number by concentrating lateral resistance in just a few bays. This resulted in both lower structural redundancy and the use of heavier structural members for the moment frames. The stringent post-Northridge design provisions prompted design practice to further evolve away from using W14 sections for columns in frames before the Northridge earthquake toward the deep, wide flange columns that are widely used at the present time (Elkady and Lignos 2015; Ozkula et al. 2017; Wu et al. 2018a, b).

Representative Steel Moment Frames

A set of steel perimeter moment frames with two-, four-, and eight-stories are designed per seismic design codes for the three selected eras. Design for wind loading is not considered to focus the study only on the evolution of seismic provisions and practices. The designs are for an office building configuration described in NIST (2010), as shown in plan in Fig. 2(a) and with the site condition used to plot Fig. 1. The eras are designated E75 (for mid-1970s designs), E90 (for early 1990s design), and E05 (for mid-2000s design) to facilitate referral to them. The frames are designated S2, S4, and S8 where the appended number is the number of stories.

E05 frames are designed with RBS connections and W24 columns (i.e., deep columns) using A992 steel, while the older frames employ WFBW connections and W14 columns with A36 and A572 Grade 50 steel for beams and columns, respectively. The yield strength of the A36 steel used in E75 and E90 frames is 296 MPa (43 ksi) and 338 MPa (49 ksi), respectively, based on the survey by Coons (1999). The major differences in seismic design and practices among the eras are summarized in Table 1, and the main characteristics of the designed frames are listed in Table 2. Full frame designs can be found in Wu (2019). Note that a design drift limit of 0.5% in the 1976 UBC is applied to E75 designs, but without the system factor modification.

Finite-Element Modeling

Modeling Approach

Following Wu et al. (2018b), detailed finite-element models (FEMs) of the moment frames are created and analyzed using Hypermesh Version 12.0 and the explicit solver implemented in LS-DYNA, respectively. The frame model is discretized using 3- and 4-node fully integrated shell elements (ELFORM 16) based

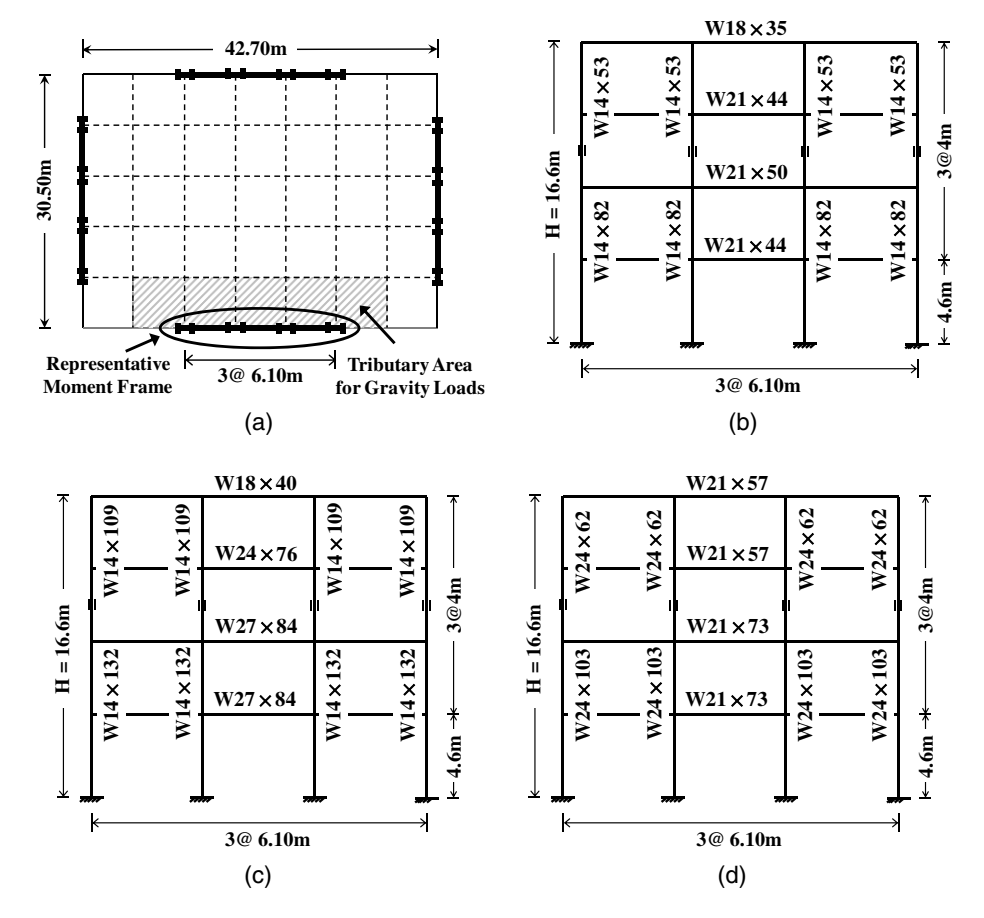


Fig. 2. (a) Typical plan configuration and elevation view of (b) S4-E75 frame; (c) S4-E90 frame; and (d) S4-E05 frame.

Table 1. Summary of major differences of the seismic design and practice between the three studied eras

Design era Mid-1970s (E75)		Early 1990s (E90)	Mid-2000s (E05)		
Frame type	Perimeter ductile MRF	Perimeter special MRF	Perimeter special MRF		
Connection type	WFBW	WFBW with supplemental web welds	RBS		
Material	A36 (beams, $F_{v} = 296 \text{ MPa}$)	A36 (beams, $F_y = 338 \text{ MPa}$)	A992		
	A572 Grade 50 (columns)	A572 Grade 50 (columns)			
Design codes	1969 AISC and 1973 UBC	1989 AISC (AISC 1989) (ASD)	AISC 360-05 (AISC 2005c)		
	(ICBO 1973)	and 1991 UBC (ICBO 1991)	(LRFD), AISC 341-05 (AISC 2005b),		
			AISC 358-05 (AISC 2005a), and ASCE 7-05		
Design drift limit	0.5%	0.25%	0.45%		
SWCB principle	N/A	Eq. (1)	Eq. (2)		
Panel zone design	Strong	Weak	Balanced		
Lateral bracing for	Only at level of top beam	At levels of both beam flanges	At levels of both beam flanges		
B/C connections	flanges	except for Eq. $(1) > 1.25$	except for Eq. $(2) > 2.0$		
Lateral bracing for beams (L_b)	Only for top beam flanges	$96r_{\rm v}$	$2500r_{v}/F_{vb}$		
Column compressive strength	N/A	$1.0P_D + 0.7P_L + 4.5P_E$	$1.2P_D + 0.5P_L + 3P_E$		

Note: P_D , P_L , and P_E = axial loads due to dead load, live load, and seismic loads, respectively. N/A = not applicable.

on the formulation published by Engelmann et al. (1989), as shown in Fig. 3. A material model (MAT153) (Huang and Mahin 2010) that employs combined isotropic/kinematic hardening and a damage model is used to represent cyclic hardening and ultralow cycle fatigue behavior in structural steel, respectively. As outlined in Wu (2019), the hardening moduli are calibrated to the true stresstrue strain model proposed by Arasaratnam et al. (2011) with the material strength of steel listed in Table 1. The damage parameters are calibrated to the experimental data in Liu and Astaneh-Asl (2000) and Engelhardt and Husain (1992), as discussed later.

The moment frames are assumed to be fully fixed at their base. Lateral bracing is simulated by preventing out-of-plane translation at key nodes [e.g., Figs. 3(b and c)]. Column flanges at the beam-to-column connections and beam flanges are laterally braced according to the requirements stipulated in the different eras, as listed in Table 1. The contributions to lateral resistance provided by the slab and gravity frames are not considered. As a result, system-wide P-Delta effects are simulated by connecting a leaning column to the frames with rigid truss members as shown in Fig. 3(a). The rigid truss member at each floor is attached to the center point

Table 2. Characteristics and collapse analysis results of representative steel moment frames

Frame ID	Design era	First-story column section	First-floor beam section	Steel weights (kN)	T_1 (s)	$\hat{S}_{a,C}(T_1, 5\%)$ (g)	β	λ_c	$P_{c,50yrs}$ (%)
Two-story	,	,		,					
S2-E75	Mid-1970s	$W14 \times 74$	$W21 \times 50$	59.2	1.30	0.65	0.47	1.40×10^{-3}	6.78
S2-E90	Early 1990s	$W14 \times 82$	$W24 \times 62$	68.5	1.18	0.78	0.48	1.17×10^{-3}	5.69
S2-E05	Mid-2000s	$W24 \times 76$	$W21 \times 44$	59.2	1.01	1.06	0.31	4.82×10^{-4}	2.38
Four-story									
S4-E75	Mid-1970s	$W14 \times 82$	$W21 \times 44$	109	2.46	0.23	0.28	2.61×10^{-3}	12.3
S4-E75-NF	Mid-1970s	$W14 \times 82$	$W21 \times 44$	109	2.46	0.28	0.29	1.59×10^{-3}	7.67
S4-E90	Early 1990s	$W14 \times 132$	$W27 \times 84$	187	1.77	0.53	0.44	1.09×10^{-3}	5.29
S4-E90-NF	Early 1990s	$W14 \times 132$	$W27 \times 84$	187	1.77	0.61	0.45	7.73×10^{-4}	3.79
S4-E05	Mid-2000s	$W24 \times 103$	$W21 \times 73$	142	1.67	0.64	0.45	8.02×10^{-4}	3.93
Eight-story									
S8-E75	Mid-1970s	$W14 \times 145$	$W24 \times 62$	297	3.74	0.12	0.28	3.67×10^{-3}	16.8
S8-E90	Early 1990s	$W14 \times 211$	$W30 \times 108$	507	2.67	0.44	0.23	3.91×10^{-4}	1.94
S8-E05	Mid-2000s	$W24 \times 162$	$W30 \times 108$	428	2.37	0.54	0.31	3.57×10^{-4}	1.77

Note: NF = fracture in pre-Northridge connections is not modeled.

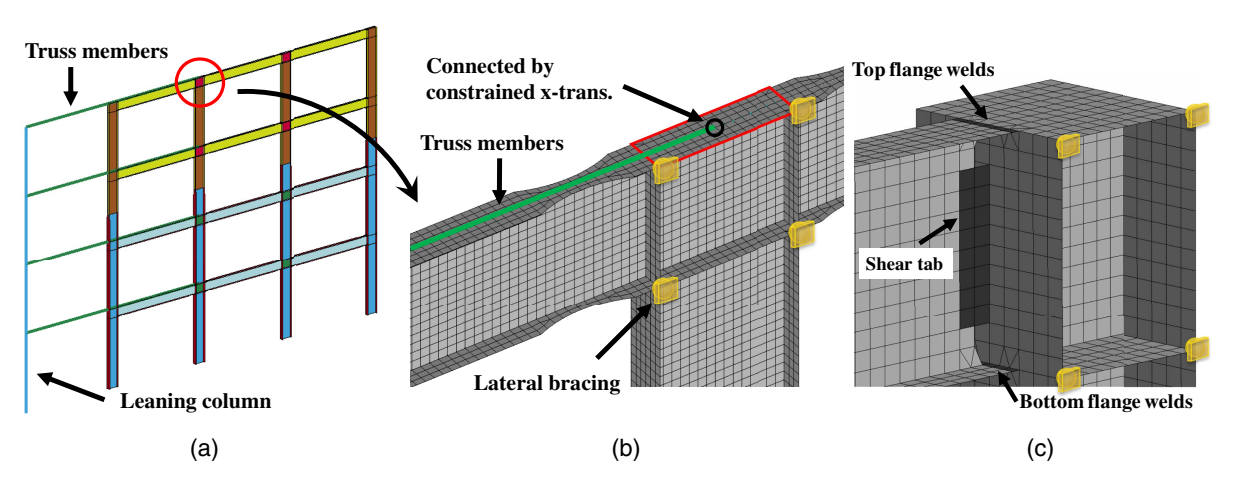


Fig. 3. Finite-element models of (a) four-story moment frame; (b) reduced beam section (RBS) connections; and (c) welded flange-bolted web (WFBW) connections.

of the continuity plate for beam top flanges with an x-translation constraint [Fig. 3(b)]. A gravity load equal to half of the building floor mass minus that distributed to the perimeter moment frame system is applied at each floor of the leaning column. A mass-proportional damping of 2.5% is assumed at the first mode period, which dominates the dynamic response of SMFs employed in this study.

Artificial geometric imperfections are not included to avoid favoring predetermined instability modes and because there is no rational way to include them throughout the frame. Sensitivity studies at the member level showed that the high numerical precision of the simulation code can accurately capture the geometric nonlinear effects associated with the minute out-of-plane deformations in the early stages of loading. These deformations create the necessary geometric imperfections for the analysis to proceed as evidenced by the favorable results in previous validation studies by the authors that included (Wu et al. 2018a) and excluded (Wu et al. 2018b) artificial initial imperfections.

As done in Wu et al. (2018b), two collapse criteria are used to detect sidesway collapse: (1) maximum story drift ratio surpasses 10%, and (2) an increase of 2% or more in story drift ratio during the 10-s window immediately after the time needed for the Arias intensity to reach 95% ($t_{IA=95\%}$) (Arias 1970). Unlike sidesway collapse, vertical progressive collapse can be clearly identified

from the deformed shape of the frame and no specific criteria are needed.

The finite-element models of the two-, four-, and eight-story frames consist of approximately 54,000, 110,000, and 240,000 elements, respectively. The simulations run on a cluster with 16 processors. The simulation time to model 30 s of real time is about 18, 42, and 90 h for the two-, four-, and eight-story frames, respectively. A total of 782 simulations are performed requiring about six months of run time.

Validation of Modeling Scheme and Calibration for Fracture Behavior

The general finite-element modeling approach used in this work has been extensively calibrated and validated in previous papers by the authors, e.g., in Fogarty and El-Tawil (2015), Fogarty et al. (2017), and Wu et al. (2018a), using available experimental data in Ozkula et al. (2017). The validation was done using component level tests and subassemblies because collapse data at the structural system level is not available. Additional calibration is sought because, unlike earlier efforts by the authors, this study models the brittle fractures in pre-Northridge connections that can occur at a small drift of 1%–2% and can have a great impact on frame responses. Parameters for brittle shear tab and beam flange weld

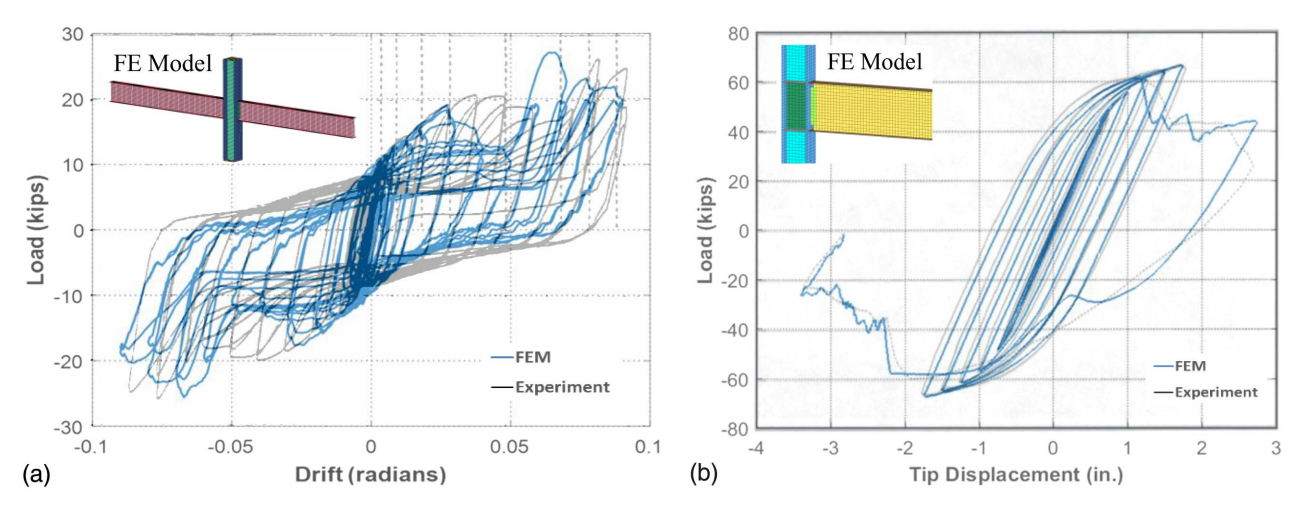


Fig. 4. Calibration results of (a) shear tab (specimen 2A; Liu and Astaneh-Asl 2000); and (b) beam flange welding (specimen 3 with supplemental web welds; Engelhardt and Husain 1992).

fracture in the WFBW connections [Fig. 3(c)] are calibrated to experimental data in Liu and Astaneh-Asl (2000) and Engelhardt and Husain (1992), respectively.

Liu and Astaneh-Asl (2000) tested 16 steel beam-column subassemblages to study the cyclic behavior of typical shear connections with and without a slab. The specimens were cross-shaped subassemblages with cyclic loads applied at the column top. The structural members and connection plates were made with A572 Grade 50 and A36 steel, respectively. Specimen 2A, which utilized a typical strong-axis shear tab without a floor slab, is selected for calibrating the material model (MAT153) used for the shear tab in the moment connections. The specimen was subjected to symmetric cyclic drift loading as specified in the AISC seismic provisions (2002). Using a trial and error approach, the best calibration results are obtained when the material model is bilinear hardening, with $F_v = 124$ MPa, tangent modulus (E_T) equalling 1% of the elastic modulus (E), and the critical damage value (D_c) equalling 0.5, as shown in Fig. 4(a). It should be noted that these parameters represent the aggregate behavior of the shear tab, including the effect of bolts and binding (contact between the beam and column flanges). The calibrated parameters are used to model the shear tabs in the E75 frames.

The parameters for modeling the beam flange welds and shear tabs in the E90 frames that have supplemental welds at the beam web connections are calibrated to the experimental data in Engelhardt and Husain (1992), who cyclically tested eight WFBW connections. The specimens were cantilever-type subassemblages with cyclic loads applied at the beam end. The beams and columns were made with A36 and A572 grade 50 steel, respectively, and an E70 welding electrode was used for welding. Because the eight specimens showed highly variable performance, all experimental results in the test program are utilized in the calibration to explore the range of D_c for beam flange welds. One of the calibrated results (for specimen 3) is shown in Fig. 4(b).

The calibration results suggest that MAT153 can still be used, but with a D_c of 0.025 to 0.04 (with an average of 0.034) and 0.002 to 0.037 (with an average of 0.021) to simulate the fracture behavior of top and bottom flange welds, respectively. The higher D_c for the top flange welds indicates better performance than the bottom flange and is consistent with the surveyed damage after the Northridge earthquake (Youssef et al. 1995). The average values of D_c are used in the computational studies below. The somewhat large randomness, which is expected given the brittle nature of

the fractures, is not considered for the sake of computational expediency.

Specimens 3 and 7 are used to calibrate the model for the shear tabs with supplemental web welds in the E90 frames. The calibration is identical to that for the Liu and Astaneh-Asl (2000) shear tabs, except for F_{ν} , which is taken as 248 MPa (36 ksi).

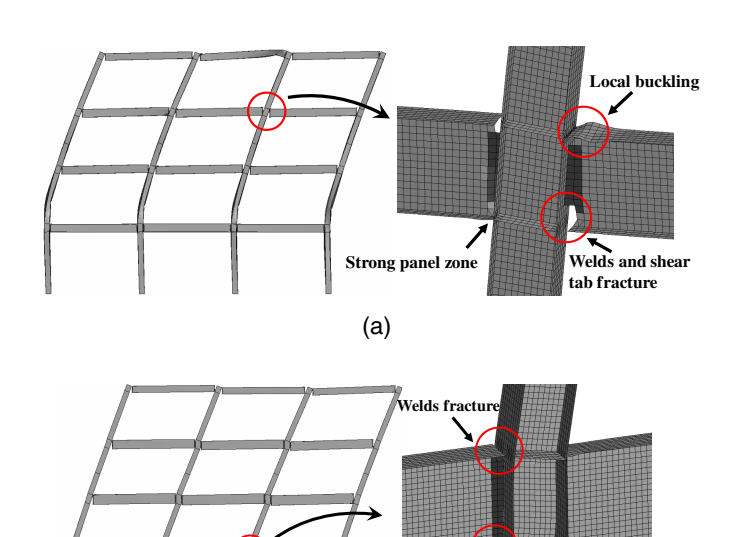
Simulation Results

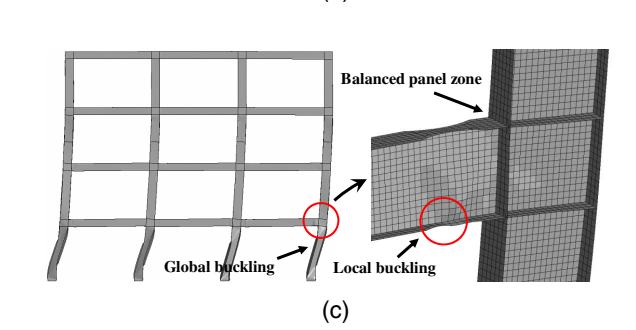
Seismic loss assessment of the moment frames (listed in Table 1) is performed using the seismic performance prediction program (SP3) (Haselton Baker Risk Group 2019), which is based on the FEMA P-58 [FEMA (2012)] methodology. The data required for the assessment, including collapse fragilities of the moment frames and building demands under earthquakes with a given intensity level, are obtained through detailed finite-element analysis using the modeling scheme described above.

Fig. 5 shows common damage modes and collapse mechanisms of moment frames designed for different eras. The S4-E75 and S4-E90 frames typically fail by a multistory sidesway mechanism [Figs. 5(a and b)], while the S4-E05 frame is more likely to collapse by a first-story mechanism due to instability of the deep columns [Fig. 5(c)]. It also can be seen that the pre-Northridge connections suffer from brittle weld fracture and deterioration of beam moment capacity [Figs. 5(a and b)]. On the other hand, the reduced beam sections in the S4-E05 frame can develop plastic hinges at the reduced region [Fig. 5(c)]. The difference in panel zone behavior due to different design philosophies also can be observed from Figs. 5, e.g., the kink in the column flanges due to a weak panel zone [Fig. 5(b)]. It is clear that the employed finite-element analysis effectively captures key aspects of the designs, e.g., panel zone design philosophy, brittle fracture in pre-Northridge connections, and global buckling of deep columns.

Collapse Capacity

The collapse fragility analyses are based on 11 ground motion records selected from the far-field record set in FEMA P695 [FEMA (2009)] and are listed in Table 3. Only 11 records are used instead of the 11 pairs (i.e., 22 records) recommended in FEMA P-58 [FEMA (2012)] as a compromise between computational expediency and the need to adequately capture ground motion variability.





nd local buckling

(b)

Weak panel zone

Fig. 5. Damage modes and collapse mechanisms of four-story moment frames from different eras: (a) S4-E75 frame subject to Northr/MUL009 record with $S_a(T_1, 5\%) = 0.31$ g; (b) S4-E90 frame subject to Hector/HEC000 record with $S_a(T_1, 5\%) = 0.73$ g; and (c) S4-E05 frame subject to Hector/HEC000 record with $S_a(T_1, 5\%) = 0.95$ g.

Table 3. Ground motion records employed in collapse fragility analysis of moment frames

No.	Event Station		Component
1	Northridge, 1994	Beverly Hills, Mulhol	9
2	Northridge, 1994	Canyon country, WLC	0
3	Duzce, 1999	Bolu	0
4	Hector Mine, 1999	Hector	0
5	Imperial Valley, 1979	Delta	262
6	Imperial Valley, 1979	El Centro Array #11	140
7	Kobe, 1995	Nishi-Akashi	0
8	Kobe, 1995	Shin-Osaka	0
9	Kocaeli, 1999	Duzce	180
10	Kocaeli, 1999	Arcelik	0
11	Landers, 1992	Yermo fire station	270

The spectral acceleration associated with collapse $[S_{a,C}(T_1,5\%)]$ of each record is then obtained by IDA (Vamvatsikos and Cornell 2002), when one of the collapse criteria is met under the scaled record. The obtained $S_{a,C}(T_1,5\%)$ values are fitted to a lognormal distribution using the collapse fragility tool provided in FEMA P-58 [FEMA (2012)] to determine the collapse fragility curve for each moment frame. Each curve is characterized by a median value

of $S_{a,C}$, $\hat{S}_{a,C}$, and dispersion, β . The mean annual frequency of collapse (λ_c) of each moment frame is computed by numerically integrating its collapse fragility curve with the seismic hazard curve associated with the site condition from USGS (2018). The collapse probability over a time frame of 50 years, $P_{c,50yrs}$, for each frame is also computed by assuming a Poisson distribution. The analysis results are summarized in Table 2, and the collapse fragility curves of the frames are plotted in Fig. 6. Note that dispersions listed in Table 2 and Fig. 6 include only the record-to-record uncertainty.

Table 2 shows that the collapse risk decreases as the seismic design codes evolved. Specifically, the E05 frames have a lower $P_{c,50vrs}$ than the corresponding E90 and E75 frames, regardless of building height. Although the E90 frames use more steel than the corresponding E05 frames (e.g., S4-E90 uses 32% more steel than S4-E05), primarily due to the use of stocky W14 sections, they have a higher collapse risk. This increased collapse risk reflects the fact that the newest generation of codes and their associated practices are more efficient. On the other hand, the E75 frames are the set of frames using the least steel. However, these frames also have the highest collapse risk. The high collapse risk is primarily attributed to the fact that there is no cap on the fundamental period used in design. The lack of a bound on the period results in smaller section sizes, greater susceptibility to P-Delta effects, and greater vulnerability to sidesway collapse at smaller drifts, in the range of 4%-5%.

The collapse risk of E05 frames appears to be consistently low and independent of building height, where $P_{c,50vrs}$ ranges from 1.8% to 3.8%. The E90 frames, on the other hand, exhibit some dependence on building height, where $P_{c.50vrs}$ is lowest for the tallest building and highest for the shortest (1.9% for S8-E90 versus 5.7% for S2-E90). This dependence mainly results from the lower seismic hazard associated with the longer period at the assumed building site and the decreased lateral resistance of the S2-E90 frame due to connection fracture. Unlike the E90 frames, the E75 frames show an opposite and clear trend. The $P_{c,50vrs}$ of the S8-E75, S4-E75, and S2-E75 frames is 16.8%, 12.3%, and 6.78%, respectively. These numbers are quite high, but comparable to $P_{c,50vrs} = 13.0\%$ computed by Hutt et al. (2019) for a 50-story building designed per 1973 UBC (ICBO 1973). The high collapse risk is directly attributed to the large flexibility of the E75 frames, which increases P-Delta effects as the frames get taller.

Another set of models is developed to investigate the effect of rehabilitation on four-story frames with pre-Northridge connections (S4-E75 and S4-E90). These frames are not allowed to exhibit brittle weld fracture, although they still account for all other important aspects of the behavior, including local and global instability. The modified frames are appended with the letters NF (no fracture), e.g., S4-E75-NF. The results are shown in Table 2 along with the results for other frames, and the collapse fragility curves of the NF frames are shown in Figs. 6(d and e).

The simulation results show that the effect of brittle fracture in pre-Northridge connections is modest in terms of collapse capacity. Not accounting for weld fracture caused the median collapse intensity, $\hat{S}_{a,C}$, to increase by about 20%, and $P_{c,50yrs}$ to decrease by about one-third for S4-75 and S4-90. One primary reason for the modest effect is that even after weld fracture occurs, the connections are still able to retain some moment capacity, as shown in Fig. 4(b), attributed to the presence of the shear tabs and the contact between the column and beam flanges, as shown in Fig. 5(b). The reduction of frame lateral stiffness caused by connection fracture also diminishes the effect by reducing the seismic demands on the frame. Although S4-E90-NF has a lower $P_{c,50yrs}$ than S4-E05, it uses much more steel, reflecting the inherent inefficiency of the E90 seismic provisions and construction practices.

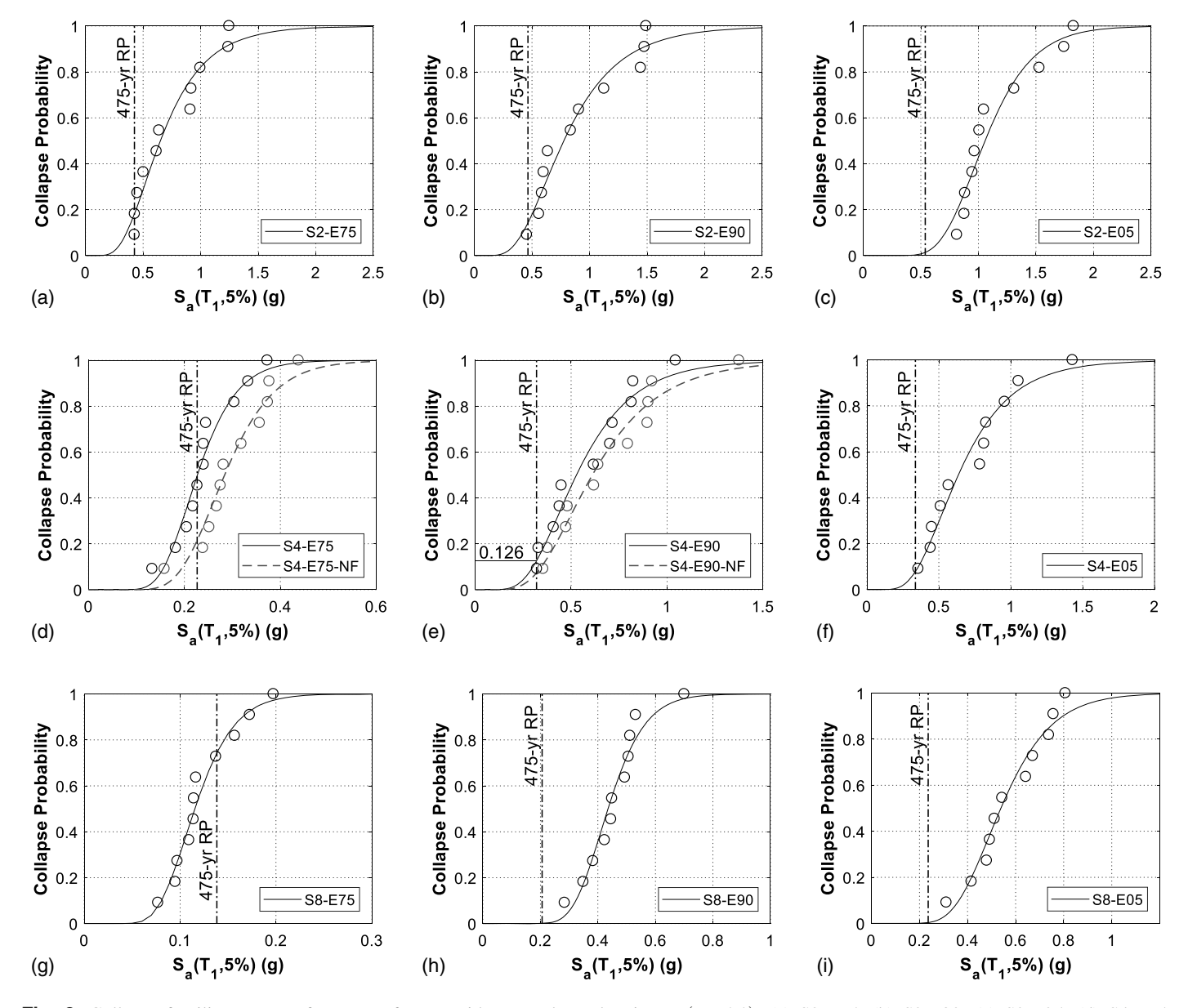


Fig. 6. Collapse fragility curves of moment frames with spectral acceleration $S_a(T_1, 5\%)$: (a) S2-E75; (b) S2-E90; (c) S2-E05; (d) S4-E75; (e) S4-E90; (f) S4-E90; (g) S8-E75; (h) S8-E90; and (i) S8-E05. 475-yr RP means 475-year return period.

A key observation from Table 2 is that none of the frames exhibit $P_{c,50yrs} < 1\%$, which is the current targeted uniform collapse risk specified by ASCE (2016) for buildings in the US. Attention is required to address the nonuniform and high $P_{c,50yrs}$ associated with steel moment frames built in different eras in communities.

Repair Cost, Repair Time, and Casualties

2,000 realizations are performed for each frame to determine key loss measures under an earthquake with a return period of 475 years. The spectral acceleration corresponding to this intensity level, $S_a(T_1,5\%)_{475}$, for each frame is plotted as a dash-dot line in Fig. 6. Corresponding to each $S_a(T_1,5\%)_{475}$ is $P_{c,Sa475}$, the collapse probability of the frame under consideration. For example, $P_{c,Sa475}$ of S4-E90 is 12.6% as shown in Fig. 6(e). $P_{c,Sa475}$ is used to determine if a frame has collapsed or not in a specific realization.

For realizations in which collapse does not occur, seven ground motion records from Table 3 are used to compute the peak story drift ratio (PSDR) and peak floor acceleration (PFA) demand parameters. These parameters are then used to estimate economic and social losses resulting from component damage. Based on the availability of the component fragility specifications provided in FEMA P-58 [FEMA (2012)], the structural and nonstructural components commonly seen in office buildings are considered in the assessment and listed in Table 4 with their fragility classification ID, name and category, demand parameter (PSDR or PFA that causes damage to the component), and number of possible damage states associated with the level of demand parameter. In the classification ID, the first letter and two numbers, the next two numbers, and the numbers after the decimal identify the category, a basic component, and variations in the basic component, respectively. For example, component B1035.011 and B1035.051 are post-Northridge RBS connection with welded web and pre-Northridge WFBW beam-column joints, respectively. Both joints are steel connections with W27 beams or smaller. Nonstructural components are assumed seismically rated only in the E05 frames

Table 4. Components considered in the resilience assessment of moment frames

Fragility classification ID	Name	Category	Demand parameter	Number of damage states
B1031.001	Steel columns	Super structure	PSDR	4
B1031.011ab		•	PSDR	4
B1031.021ab			PSDR	3
B1035.001	Steel connections	Super structure	PSDR	3
B1035.002		aup of an artificial	PSDR	3
B1035.011			PSDR	3
B1035.012			PSDR	3
B1035.021			PSDR	3
B1035.031			PSDR	3
B1035.041			PSDR	5
B1035.042			PSDR	5
B1035.042 B1035.051			PSDR	5
B1035.051 B1035.052			PSDR	5
	Enterior well construction	Enterior en el como		
B2011.201a	Exterior wall construction	Exterior enclosure	PSDR	2
B2011.201b	G	F	PFA	1
B2022.001	Curtain walls	Exterior enclosure	PSDR	2
C1011.011a	Fixed partitions	Interior construction	PSDR	3
C2011.001	Regular stairs	Stairs	PSDR	3
C3011.001a	Wall partitions finishes	Interior finishes	PSDR	1
C3032.001abcd	Suspended ceilings	Interior finishes	PFA	3
C3032.003abcd			PFA	3
C3034.001	Independent pendant lighting	Interior finishes	PFA	1
C3034.002			PFA	1
D1014.011	Traction and hydraulic elevators	Conveying	PFA	4
D2021.012a	Potable water service	Plumbing	PFA	2
D2021.012b			PFA	2
D2021.013a			PFA	2
D2021.013b			PFA	1
D2021.022a			PFA	2
D2021.023a			PFA	2
D2021.023b			PFA	2
D2022.012a	Hot water service	Plumbing	PFA	2
D2022.012b			PFA	2
D2022.013a			PFA	2
D2022.013b			PFA	1
D2022.022a			PFA	2
D2022.023a			PFA	2
D2022.023b			PFA	2
D2031.022a	Waste piping	Plumbing	PFA	1
D2031.022b	waste piping	Tumbing	PFA	2
D2031.0220			PFA	1
D2031.023a D2031.023b			PFA	1
D3031.011abcd	Chilled seter systems	HVAC	PFA	
D3031.013cfil	Chilled sater systems	пvAC	PFA	1 3
D3031.021abcd			PFA	1
D3031.023cfil	A in distribution and an	IDAC	PFA	3
D3041.011c	Air distribution systems	HVAC	PFA	2
D3041.012c	- ·		PFA	2
D3052.011abcd	Package units	HVAC	PFA	2
D3052.013cfil			PFA	4
D4011.022a	Sprinkler water supply	Fire protection	PFA	2
D4011.023a			PFA	2
D4011.032a			PFA	2
D4011.053a			PFA	2
D5012.013a	Low tension service and dist.	Electrical	PFA	1
D5012.013d			PFA	3
D5012.021abcd			PFA	1
D5012.023cfil			PFA	3

because the detailed seismic design requirements of those components were not specified until the 2000 International Building Code (IBC) (ICC 2000).

For each frame, the computed losses include mean repair cost (direct economic loss), mean repair time (indirect economic loss),

and mean casualties (social loss). The repair time is calculated by assuming that only one floor can be repaired at a time, i.e., serial repair time. The casualties in each realization are calculated by the population model combined with the casualty rate from falling hazard of components (if collapse does not occur) or building

Table 5. Loss estimation of representative moment frames and retrofitted frames under an earthquake with a return period of 475 years

	Seismically rated	Total		Mean repair cost ^a			Mean	Mean casualties (number of people/floor)		
Frame ID	nonstructural components	replacement cost (US Dollars)	$P_{c,Sa475} \ (\%)$	Structural (%)	Nonstructural (%)	Total (%)	repair time (days)	Falling hazard	Collapse	Total
S2-E75	N	7.06M	18.2	8.2	13.5	39.9	108	0.83	1.08	1.91
S2-E90	N	7.06M	14.2	5.5	12.8	32.5	86	0.63	0.88	1.52
S2-E05	Y	7.06M	1.4	1.7	8.7	11.8	22	0.06	0.08	0.14
S4-E75	N	14.1M	50.0	3.2	6.5	59.7	277	0.39	3.06	3.46
S4-E90	N	14.1M	12.6	3.6	10.8	27.0	114	0.69	0.76	1.45
S4-E05	Y	14.1M	7.9	2.4	7.0	17.3	74	0.08	0.48	0.56
S8-E75	N	28M	74.7	0.9	2.2	77.8	461	0.13	4.52	4.66
S8-E90	N	28M	0.7	3.5	10.5	14.7	104	0.92	0.04	0.97
S8-E05	Y	28M	0.3	0.5	5.2	6.0	44	0.02	0.02	0.04
S4-E75-NS	Y	14.1M	50.0	3.2	5.1	58.3	271	0.11	3.08	3.19
S4-E75-NF	N	14.1M	21.6	3.8	9.2	34.6	154	0.46	1.29	1.75
S4-E75-NF-NS	Y	14.1M	21.6	3.7	7.0	32.3	146	0.13	1.31	1.44
S4-E90-NS	Y	14.1M	12.6	3.7	7.9	24.2	106	0.10	0.78	0.88
S4-E90-NF	N	14.1M	7.3	2.9	11.1	21.3	85	0.67	0.44	1.11
S4-E90-NF-NS	Y	14.1M	7.3	3.0	8.3	18.6	76	0.10	0.44	0.54

^aExpressed as a percentage of building total replacement cost.

collapse (if collapse occurs). The mean casualties are normalized by the number of floors to facilitate comparisons between buildings with different heights. Reparability associated with residual drift is not considered. The loss estimation results, including $P_{c,Sa475}$, mean repair cost contributed by structural and nonstructural components, and mean casualties contributed by falling components and building collapse are summarized in Table 5, where it is clear that newer frames have better overall performance indicators.

Table 5 shows that the E05 frames not only require much less repair cost and time to physically recover, but also have much less social impact on communities than their older counterparts. This result is not surprising because these frames, designed to the latest specification and practices, have the lowest collapse risk. Nevertheless, collapse risk paints only part of the overall loss picture. Building size is another important consideration. For example, S8-E90 has the lowest $P_{c,Sa475}$ among all of the E90 frames, but the worst performance indicators (specifically, economic and social losses) because of its size.

While the detailed assessment results are not shown, the major factors contributing to the estimated losses are the collapse probability of the frames at the given intensity level, i.e., $P_{c,Sa475}$, fragility of the moment connections, and seismic rating of nonstructural components. The influence of $P_{c,Sa475}$ on repair cost is evident in the proportional relationship between them. For example, the $P_{c.Sa475}$ and repair cost of S4-E75 frame is 50.0% and 59.7%, respectively, and the $P_{c,Sa475}$ and repair cost of S8-E75 frame is 74.7% and 77.8%, respectively. The effect of fragility of the moment connections and seismic rating of nonstructural components can be observed by comparing the losses of S8-E90 to S8-E05. Although these two frames both have a low $P_{c,Sa475}$, S8-E90 has more than double the repair cost and time and much higher casualties than S8-E05. The former effects (repair cost and time considerations) are due to the pre-Northridge connections and non-seismically rated nonstructural components, while the latter effect (casualties) is attributed to the then-prevalent use of nonseismic pendant lighting, which are prone to fail during an earthquake. The above observation suggests that not only does the collapse fragility of older frames need to be improved, but also the seismic rating of its nonstructural components in order to minimize the seismic losses incurred by communities.

Strategies to Reduce Seismic Losses in Communities

Seismic retrofit is expensive. As a result, most building owners will not embark on a rehabilitation program unless required by authorities, e.g., through an ordinance. The results of the simulations conducted in this paper can provide insight into which retrofit strategies most influence the losses of communities containing older steel moment frame buildings. A seismic loss assessment similar to that done in this study is performed on the S4-E75 and S4-90 frames by assuming that they have already been upgraded to have: (1) connection welds that are not prone to brittle fracture, and/or (2) seismically rated nonstructural components in certain categories, specifically stairs, ceilings, lighting, piping, HVAC, and electrical equipment. In the following discussions, frames with upgraded nonstructural components are designated with the letters NS, e.g., S4-E75-NS. As noted earlier, frames with upgraded connection welds are designated with NF. Frames with both NS and NF have been retrofitted along both fronts, e.g., S4-E75-NF-NS. Analyses are then conducted to shed light on how the NS, NF, and combined NS/NF strategies affect the performance indicators of the frames.

As shown in Table 5, unlike its relatively moderate impact on collapse capacity, fracture of pre-Northridge connections has a more severe effect on losses for the four-story frames. While the increase in demand parameters is only 10%, as also indicated in Luco and Cornell (2000), the change in collapse probability, and therefore loss, is influential for the given hazard level. For example, upgrading connections for S4-E75 (i.e., S4-E75-NF) can significantly decrease $P_{c,Sa475}$ from 50% to 21.6% and substantially lowers the total mean repair cost (drops from 59.7% to 34.6%). The mean casualties are also reduced by half (from 3.46 to 1.75) because the casualties due to collapse are largely avoided. The effect of upgraded connections on S4-E90 are much less significant because of the frame's lower $P_{c,Sa475} = 12.6\%$ (versus 50% for S4-E75). For S4-E90, the total mean repair cost and casualties per floor decline from 27.0% and 1.45 to 21.3% and 1.11, respectively, when the NF repair is applied (i.e., S4-E90-NF).

The NS approach has only a small effect on the economic losses for S4-E90 (Table 5) because the repair cost is mostly contributed by collapse and nonstructural components that do not have the option for seismically rated upgrade. For example, the mean repair

cost of S4-E90 drops from 27.0% to 24.2% by upgrading to seismically rated nonstructural components (S4-E90-NS). Applying both approaches (S4-E90-NF-NS) is more effective and reduces the mean repair cost to 18.6%. The effect on casualties is more substantial, where applying both NF and NS reduces the mean number of casualties from 1.45 to 0.54. Similar trends can be seen for the S4-E75 frame, where the NS approach only reduces the mean repair cost by a small amount (from 59.7% to 58.3%) due to fact that half of realizations predict collapse, i.e., $P_{c,Sa475} = 50.0\%$. Applying NS and NF reduces the mean repair cost further to 32.3%. This number is still higher than the 30% maximum repair cost that owners would typically consider after major events before deciding to abandon a building (Kim 2015) and suggests that most owners would balk at a retrofit of this sort. However, a closer look at the effect of retrofit on mean casualties per floor suggests that rehabilitation could be quite effective if the performance objective were just focused on saving lives (the mean casualties per floor drop from 3.46 to 1.44 for S4-E75 versus S4-E75-NF-NS, respectively).

A detailed analysis of the upgrade costs indicates that seismically upgrading certain components could be quite effective in improving loss measures. For example, upgrading stairs and HVAC systems contribute to 89% of the reduction in mean repair cost between S4-E90 and S4-E90-NS (i.e., as shown in Tables 5, 27.0%–24.2% = 2.8% reduction). Nonseismic independent pendant lighting (C3034.001) is a key source of casualties due to the falling hazard and upgrading those in the S4-E90 frame can eliminate 40% of the mean casualties per floor.

The above discussion demonstrates the complexity of proposing and enforcing meaningful seismic upgrade policies and ordinances. It indicates that judiciously selected requirements can have a substantial effect on seismic losses but with low to modest implementation cost. The study highlights that simulations of the sort done here can serve as a basis for cost-optimizing community-wide decisions regarding reduction in seismic losses through mandated policies.

Limitations of the Study

Some key assumptions and limitations of the study should be noted. Because the focus of this study is on the influence of the evolution of seismic design provisions, the design of representative steel moment frames does not consider wind loading and may reflect a greater seismic risk than real buildings due to potentially smaller section sizes. Second, the moment frame models do not include the effect of soil-structure interaction (SSI) nor contribution of the slab and gravity frames, which may potentially influence the seismic risk and repair costs associated with the beam-to-column connections. Third, the use of only 11 ground motion records due to the large computational cost associated with the high-fidelity models may underestimate the ground motion variability. Moreover, the lack of consideration of irreparability in the seismic loss assessment may underestimate the losses of steel moment frames considered in this study. However, realignment and repair cost of structures for different degrees of residual drift is currently not well-established or available. Finally, the findings in this study are drawn from a limited set of frames with a specific configuration, located at a specific site, and require a more comprehensive set of simulations to be generalized.

Conclusion

This paper presents a computational study that systemically investigates the effect of seismic design evolution on seismic risk of steel

moment frames and their influence on seismic losses of communities. A set of steel perimeter moment frames with three different heights are assumed in Santa Monica, California, and designed using seismic design codes from three eras spanning the past half century. The three eras, i.e., mid-1970s, early 1990s, and mid-2000s, represent the major differences in the evolution of seismic design and practice, including material properties, connection types, seismic design force, and panel zone design philosophy. High-fidelity finite-element models capable of capturing fracture and instabilities in the steel structures are employed to reflect the differences. Within the limitations and assumptions of the study, the following conclusion can be drawn from the collapse analysis and seismic loss assessment of the set of steel moment frames:

- The collapse capacity of the moment frames increases as seismic design provisions evolved. Nevertheless, even the frames built according to the latest seismic provisions exhibit a collapse probability in 50 years larger than 1%, which is the expected collapse risk targeted by current seismic design maps. The non-uniform and higher collapse risk posed to communities by steel moment frames built in different eras requires attention.
- While the mid-2000s frames have consistently low collapse risk regardless of the building height, the collapse risk of mid-1970s and early 1990s frames are negatively and positively affected by the height due to large flexibility and lower seismic hazard associated with longer periods, respectively. These trends suggest that taller, older steel moment frames present higher seismic risk to communities. The fact that the early 1990s frames use 20% more steel than the mid-2000s frames but have a higher collapse risk reflects the inefficiency of the early 1990s design codes.
- Under an earthquake with a return period of 475 years, newer frames show better performance and lead to less economic (repair cost and time) and social (casualties) losses experienced by communities. The tallest buildings have the largest estimated loss, even though they have the lowest collapse risk because of their great bulk.
- The key factors contributing most to the performance measures
 of steel moment frames are collapse probability at a given intensity level, fragility of moment connections, and seismic rating of
 nonstructural components. The assessment results suggest that
 all three factors need to be improved to minimize the seismic
 losses incurred by communities.
- The effect of brittle fracture in the welds of pre-Northridge connections (E75 and E90 frames) on frame collapse capacity is modest for the four-story frames. Even after fracture, the connections can still retain some moment capacity because of the presence of the shear tab and the contact between column flanges and beam flanges. Unlike with collapse capacity, weld fracture has a larger influence on losses. Rehabilitation of connection welds can reduce the losses by nearly half when the frame is vulnerable to collapse under a given earthquake.
- For the four-story frames, applying both retrofit of pre-Northridge connections to prevent brittle weld fracture and upgrade of nonstructural components is more effective and able to largely lower both economic social losses because this strategy addresses three major factors, collapse probability, fragility of moment connections, and seismic rating of nonstructural components. Among the upgraded nonstructural components, stairs and HVAC system are more critical to reducing repair cost, while nonupgraded independent pendant lighting is a key source of casualties due to falling hazard.

The conclusions drawn above are from a limited set of frame studies. Simulations of other frame configurations are needed to generalize the results. Nevertheless, the study demonstrates the complexity of proposing and enforcing meaningful seismic upgrade policies and ordinances. It indicates that judiciously selected requirements could have a substantial effect on seismic losses but with low to modest implementation cost. The study also highlights that simulations of the sort done here can serve as a basis for cost-optimizing community-wide decisions regarding reduction in seismic losses through mandated policies.

Data Availability Statement

All data, models, and code generated or used during the study appear in the published article.

Acknowledgments

This work was supported by the University of Michigan and US NSF grant numbers ACI-1638186. An academic license of the SP3 Design (www.hbrisk.com) was used in the performance of this work. Any opinions, findings, conclusions, and recommendations expressed in this paper are those of the authors and do not necessarily reflect the views of the sponsor.

References

- AISC. 1961. Specification for the design, fabrication, and erection of structural steel for buildings. Chicago: AISC.
- AISC. 1969. Specification for the design, fabrication, and erection of structural steel for buildings. Chicago: AISC.
- AISC. 1989. Specification for structural steel buildings, allowable stress design and plastic design. Chicago: AISC.
- AISC. 1990. Seismic provisions for structural steel buildings. Chicago: AISC.
- AISC. 1997. Seismic provisions for structural steel buildings. Chicago: AISC.
- AISC. 2002. Seismic provisions for structural steel buildings. ANSI/AISC 341. Chicago: AISC.
- AISC. 2005a. Prequalified connections for special and intermediate steel moment frames for seismic applications. ANSI/AISC 358. Chicago: AISC.
- AISC. 2005b. Seismic provisions for structural steel buildings. ANSI/AISC 341. Chicago: AISC.
- AISC. 2005c. Specification for structural steel buildings. ANSI/AISC 360. Chicago: AISC.
- AISC. 2010. Seismic provisions for structural steel buildings. ANSI/AISC 341. Chicago: AISC.
- Arasaratnam, P., K. S. Sivakumaran, and M. J. Tait. 2011. "True stress-true strain models for structural steel elements." *ISRN Civ. Eng.* 2011: 1–11. https://doi.org/10.5402/2011/656401.
- Arias, A. 1970. "A measure of earthquake intensity." In Seismic design for nuclear power plants, edited by R. J. Hansen, 438–483. Cambridge, MA: MIT Press.
- ASCE. 1998. Minimum design loads for buildings and other structures. ASCE/SEI 7. Reston, VA: ASCE.
- ASCE. 2005. Minimum design loads for buildings and other structures. ASCE/SEI 7. Reston, VA: ASCE.
- ASCE. 2016. Minimum design loads for buildings and other structures. ASCE/SEI 7-05. Reston, VA: ASCE.
- Bartlett, F. M., R. J. Dexter, M. D. Graeser, J. J. Jelinek, B. J. Schmidt, and T. V. Galambos. 2003. "Updating standard shape material properties database for design and reliability." Eng. J. AISC 40 (1): 2–14.
- Coons, R. G. 1999. "Seismic design and database of end-plate and T-stub connections." M.S. thesis, Dept. of Civil and Environmental Engineering, Univ. of Washington.
- Dobry, R., R. D. Borcherdt, C. B. Crouse, I. M. Idriss, W. B. Joyner, G. R. Martin, M. S. Power, E. E. Rinne, and R. B. Seed. 2000. "New site coefficients and site classification system used in recent building seismic code provisions." *Earthquake Spectra* 16 (1): 41–67. https://doi.org/10.1193/1.1586082.

- Elkady, A., and D. Lignos. 2015. "Analytical investigation of the cyclic behavior and plastic hinge formation in deep wide-flange steel beam-columns." *Bull. Earthquake Eng.* 13 (4): 1097–1118. https://doi.org/10.1007/s10518-014-9640-y.
- Ellingwood, B. R., O. C. Celik, and K. Kinali. 2007. "Fragility assessment of building structural systems in Mid-America." *Earthquake Eng. Struct. Dyn.* 36 (13): 1935–1952. https://doi.org/10.1002/eqe.693.
- Engelhardt, M. D., and A. S. Husain. 1992. Cyclic tests on large scale steel moment connections. Rep. No. PMFSEL 92-2. Austin, TX: Univ. of Texas.
- Engelmann, B. E., R. G. Whirley, and G. L. Goudreau. 1989. "A simple shell element formulation for large-scale elastoplastic analysis." In Analytical and computational models of shells, edited by A. K. Noor, T. Belytschko, and J. C. Simo. New York: ASME.
- FEMA. 2000a. Recommended seismic design criteria for new steel moment frame buildings. Rep. No. FEMA-350. Washington, DC: FEMA.
- FEMA. 2000b. State of the art report on systems performance of steel moment frames subjected to earthquake ground shaking, SAC steel project. Rep. No. FEMA-355C. Washington, DC: FEMA.
- FEMA. 2009. Quantification of building seismic performance factors. Rep. No. FEMA-P695. Washington, DC: FEMA.
- FEMA. 2010. Multi-hazard loss estimation methodology, earthquake model, HAZUS-MH MR5, technical manual. Washington, DC: FEMA.
- FEMA. 2012. Seismic performance assessment of buildings. Rep. No. FEMA-P-58. Washington, DC: FEMA.
- Fogarty, J., and S. El-Tawil. 2015. "Collapse resistance of steel columns under combined axial and lateral loading." J. Struct. Eng. 142 (1): 04015091. https://doi.org/10.1061/(ASCE)ST.1943-541X.0001350.
- Fogarty, J., T.-Y. Wu, and S. El-Tawil. 2017. "Collapse response and design of deep steel columns subjected to lateral displacement." J. Struct. Eng. 143 (9): 04017130. https://doi.org/10.1061/(ASCE)ST.1943-541X .0001848.
- Haselton Baker Risk Group. 2019. "Seismic performance prediction program." Accessed January 31, 2019. https://www.hbrisk.com/.
- Huang, Y., and S. A. Mahin. 2010. Simulating the inelastic seismic behavior of steel braced frames including the effects of low-cycle fatigue. Rep. No. PEER 2010/104. Berkeley, CA: Pacific Earthquake Engineering Research Center, Univ. of California at Berkeley.
- Hutt, C. M., T. Rossetto, and G. Deierlein. 2019. "Comparative risk-based seismic assessment of 1970s vs modern tall steel moment frames." J. Constr. Steel Res. 159 (Aug): 598–610. https://doi.org/10.1016/j .jcsr.2019.05.012.
- ICBO (International Conference of Building Officials). 1961. *Uniform building code*. Whittier, CA: ICBO.
- ICBO (International Conference of Building Officials). 1967. *Uniform building code*. Whittier, CA: ICBO.
- ICBO (International Conference of Building Officials). 1970. *Uniform building code*. Whittier, CA: ICBO.
- ICBO (International Conference of Building Officials). 1973. Uniform building code. Whittier, CA: ICBO.
- ICBO (International Conference of Building Officials). 1976. *Uniform building code*. Whittier, CA: ICBO.
- ICBO (International Conference of Building Officials). 1988. Uniform building code. Whittier, CA: ICBO.
- ICBO (International Conference of Building Officials). 1991. Uniform building code. Whittier, CA: ICBO.
- ICBO (International Conference of Building Officials). 1997. *Uniform building code*. Whittier, CA: ICBO.
- ICC (International Code Council). 2000. International building code. Whittier, CA: ICC.
- Kim, J. H. 2015. "Quantitative fanalysis of factors influencing postearthquake decisions on concrete buildings in Christchurch." M.S. thesis, Dept. of Civil Engineering, Univ. of British Columbia.
- Kircher, C. A. 2003. "Earthquake loss estimation methods for welded steel moment-frame buildings." *Earthquake Spectra* 19 (2): 365–384. https://doi.org/10.1193/1.1572171.
- Liu, J., and A. Astaneh-Asl. 2000. Experimental and analytical studies of the cyclic behavior of simple connections in steel frame buildings. Rep. No. UCB/CEE-STEEL-2000/01. Berkeley, CA: Univ. of California, Berkeley.

- Luco, N., and C. A. Cornell. 2000. "Effects of connection fractures SMRF seismic drift demands." J. Struct. Eng. 126 (1): 127–136. https://doi.org/10.1061/(ASCE)0733-9445(2000)126:1(127).
- NIST. 2010. Evaluation of the FEMA P695 methodology for quantification of building seismic performance factors. NIST GCR 10-917-8. Gaithersburg, MD: NIST.
- Noroozinejad Farsangi, E., F. Hashemi Rezvani, M. Talebi, and S. A. H. Hashemi. 2016. "Seismic risk analysis of steel-MRFs by means of fragility curves in high seismic zones." Adv. Struct. Eng. 17 (9): 1227–1240. https://doi.org/10.1260/1369-4332.17.9.1227.
- Ozkula, G., J. Harris, and C.-M. Uang. 2017. "Observations from cyclic tests on deep, wide-flange beam-columns." *Eng. J.* 54 (1): 45–59.
- Roeder, C. W. 2000. State of the art report on connection performance. FEMA Rep. No. 355D. Washington, DC: FEMA.
- SEAOC (Structural Engineers Association of California) Seismology Committee. 2009. SEAOC blue book compilation 2009. Sacramento, CA: SEAOC.
- Stillmaker, K., X. Lao, C. Galassoc, and A. Kanvinde. 2017. "Column splice fracture effects on the seismic performance of steel moment frames." J. Constr. Steel Res. 137 (1): 93–101. https://doi.org/10.1016/j.jcsr.2017.06.013.

- Uang, C. M., and M. Bruneau. 2018. "State-of-the-art review on seismic design of steel structures." J. Struct. Eng. 144 (4): 03118002. https://doi .org/10.1061/(ASCE)ST.1943-541X.0001973.
- USGS. 2018. "Unified hazard tool." Accessed January 31, 2019. https://earthquake.usgs.gov/hazards/interactive/.
- Vamvatsikos, D., and C. A. Cornell. 2002. "Incremental dynamic analysis." Earthquake Eng. Struct. Dyn. 31 (3): 491–514. https://doi.org/10.1002/eqe.141.
- Wu, T.-Y. 2019. "Seismic collapse resilience of buildings with steel moment resisting frames." Ph.D. dissertation, Dept. of Civil and Environmental Engineering, Univ. of Michigan.
- Wu, T.-Y., S. El-Tawil, and J. McCormick. 2018a. "Highly ductile limits for deep steel columns." *J. Struct. Eng.* 144 (4): 04018016. https://doi.org /10.1061/(ASCE)ST.1943-541X.0002002.
- Wu, T.-Y., S. El-Tawil, and J. McCormick. 2018b. "Seismic collapse response of steel moment frames with deep columns." J. Struct. Eng. 144 (9): 04018145. https://doi.org/10.1061/(ASCE)ST.1943-541X .0002150.
- Youssef, N., D. Bonowitz, and J. Gross. 1995. A survey of steel moment resisting frame buildings affected by the 1994 Northridge Earthquake. Rep. No. NISTIR 5625. Gaithersburg, MD: NIST.